

The Eurasia Proceedings of Science, Technology, Engineering and Mathematics (EPSTEM), 2025

Volume 37, Pages 676-688

ICEAT 2025: International Conference on Engineering and Advanced Technology

Buckling Analysis of Corrugated Plate Fuselage Under Uniform Pressure Loading Condition

Muhammad Mubashir

University of Engineering and Technology Lahore

Mohsin Akhter

University of Engineering and Technology Lahore

Qasim M. Turki

University of Al-Qadisiyah

Alaa Raad Hussein

University of Baghdad

Anas Asim

National Textile University

Shoaib Ur-Rehman

University of Engineering and Technology Lahore

Abstract: The optimization of fuselage structures is key focus in domain of aerospace engineering to ensure the weight efficiency, safety and resistance to buckling and deformation under different loading conditions. This study evaluated the static stress and buckling behavior of fuselage section using Finite Element Analysis (FEA). Three distinct fuselage configurations were employed: Skin, Skin with Bulkheads, and Skin with both Bulkheads and Stringers. Titanium alloy Ti-6Al-2Nb was used in all the configurations because of its stability and high strength to weight ratio. FEA using ANSYS was performed to evaluate deformation, stress and buckling performance under uniformly distributed pressure loading. The results show that including stringers significantly improves the structural performance. Design 3, including of bulkheads and stringers, revealed lowest deformation (54.46 mm), lowest von Mises stress (400 MPa) along with highest FoS (2.32) and buckling multiplier (>1). Thus, the study demonstrates that adding appropriate internal reinforcement elements in fuselage structures enhance load bearing capacity and structural stability.

Keywords: Aircraft fuselage, Buckling, Equivalent stress, Stiffeners, Finite element analysis, Stress analysis

Introduction

Fuselage is serving to accommodate the payload such as fuel, cargo and passengers and is one of the critical load bearing components in any aircraft. It transmits the Aerodynamic and inertial forces throughout the airframe. Optimize design of fuselage is significant to meet the increasing performance criteria including of safety and weight reduction. The application of corrugated plate structures in fuselage skins has gained attention because of the favorable mechanical behavior and enhanced buckling resistance. Veer et al. (2022) reported that use of corrugated plate fuselages can significantly change the stress distribution in shear, bending and axial loads.

- This is an Open Access article distributed under the terms of the Creative Commons Attribution-Noncommercial 4.0 Unported License, permitting all non-commercial use, distribution, and reproduction in any medium, provided the original work is properly cited.

- Selection and peer-review under responsibility of the Organizing Committee of the Conference

Performance of fuselage with corrugated geometries improved stiffness and buckling phenomena as highlighted by Karthick et al. (2013).

Finite element analysis of wing configurations has been performed in academic research (Peruru & Abhisetti, 2017). Wing structural analysis under application of external loads and depending on the mesh size is also studied by Satyanarayana Gupta et al. (2017). Several studies have also been made in modeling the fuselage structures (Buehrle, Fleming, Pappa, & Grosveld, 2000; Hussain, Chandan, & Technology, 2016; Karthick et al., 2013; Raju, Suresh, Ramesh, & Hathiram, 2018). However, limited research has done to determine the mechanical performance under different stiffening configurations in corrugated fuselages. Prior studies (Raju et al., 2018; Veeranjaneyulu et al., 2022) focused on global response of fuselage structures lacking buckling behavior.

The study is aim to present a comprehensive static and buckling analysis of corrugated fuselage structures applying ANSYS FEM simulations. Fuselage model is referenced from (Veeranjaneyulu et al., 2022; Wang et al., 2021) studies and analyzed under three different configurations such as; corrugated skin only (Design 1), Skin with bulkheads (Design 2), and Skin with bulkheads and longitudinal stringers (Design 3). Titanium alloy Ti-6Al-2Nb is used for all the configurations because of the widely used applications in aerospace and is known for its high-strength to weight ratio (Madier, 2020). The structural performance of each design is evaluated considering stress distribution, equivalent stain, Factor of Safety (FoS) and buckling load analysis. The study provides valuable insights to designers to enhance the structural efficiency using internal stiffeners. The mesh convergence and load path sensitivity presented in this work improve the simulation accuracy and a reference guide for future parametric studies on fuselage design.

Method

Governing Equations

A buckling is commonly referred as instable or rapid sideward deformation of the structure under applied load that occurred due to sudden conversion of internal energy of the structure to kinetic energy (Madenci & Guven, 2015). The mathematically form of this energy conversion is given below

$$[m][\ddot{x}] + [k][x] = [F(t)] \quad (1)$$

In equation (1), the terms $[m][x]$ and $[k]$ represents the kinetic and potential energies of the structure respectively. While, $[F(t)]$ is the external applied force on structure that creates the conversion between energies. Commonly for buckling analysis the main point of concern is the estimation of buckling load that mostly relates to static stress analysis of ANSYS so the equation (1) can be simplified as follow for the starting point.

$$[k][x] = [F(t)] \quad (2)$$

The above matrix is solved in static analysis module of ANSYS and compute the values of stress based on initial applied load on structure and creates a stress stiffening matrix $[S]$. This stress stiffening matrix $[S]$ is then transfer to the eigenvalue buckling module of ANSYS where it uses the equation (3) shown below, for computation of buckling load factor.

$$[k_t] + \theta_i[S][\omega_i] = 0 \quad (3)$$

While, k_t is the total tangent stiffness matrix that is different from initial stiffens matrix $[k]$ used in equation (2), θ_i is the load multiplier or factor obtained after the solving above equation in ANSYS. ω_i is the mode shape corresponding to each multiplier.

Fuselage CAD Modeling

The CAD modelling of the fuselage was completed using the commercially available CAD software (Solid works 2018). The geometric dimensions of the fuselage has been taken from the literature studies; B373 fuselage (Veeranjaneyulu et al., 2022; Wang et al., 2021).

Design Configurations

Three different CAD designs, listed in Table 1, were developed for evaluating the failure parameters through numerical modelling. The overview of the CAD configurations are shown in Figure 1. The number of bulkheads and longitudinal stringer are taken as 21 and 4 respectively. Total span of skin is taken 12180 mm and the thickness of bulkhead and ribs is 150 mm. The design 1 is only skin without any internal member. The design 2 incorporates the bulkheads only while the design 3 have both bulkheads and longitudinal small stringers.

Table 1. Design configurations used for fuselage analysis

Design #	Skin	Bulkhead	Stringer
1	✓	✗	✗
2	✓	✓	✗
3	✓	✓	✓

Fuselage Material Assignment

Titanium alloy Ti-6AL-2NB was chosen for current study owing to its high strength-to-weight ratio and common application in aerospace industry. The relevant properties of the material are listed in Table 2.

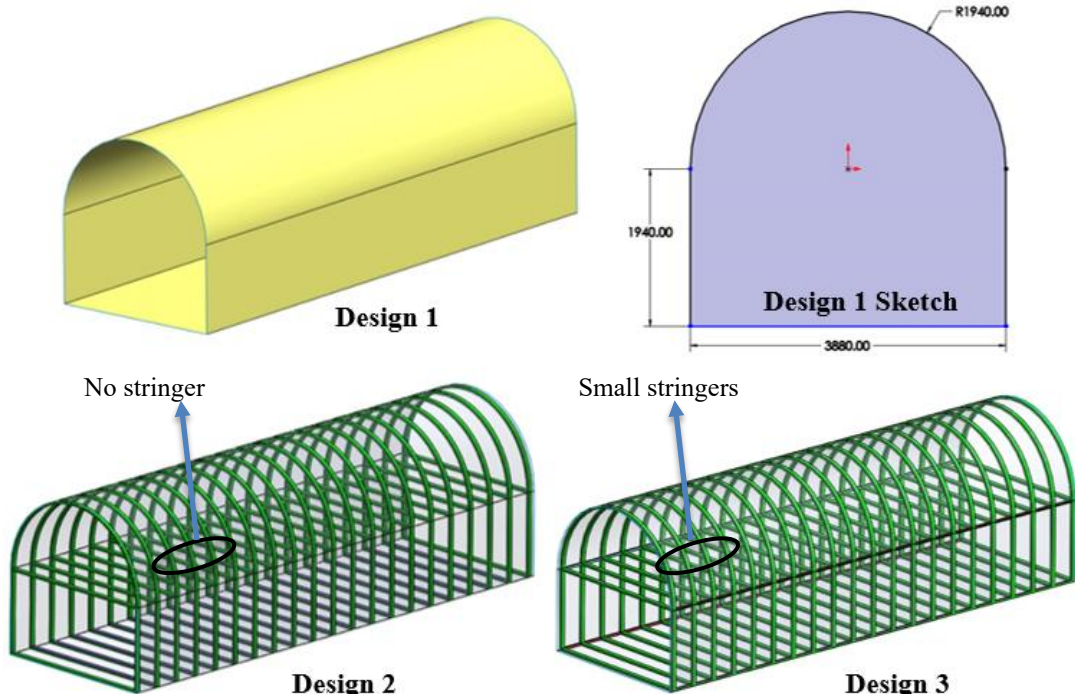


Figure 1. CAD designs prepared for conducting buckling analysis (Fuselage)

Table 2. Material properties of titanium alloy used for analysis

Parameter	Symbol	Magnitude	Unit
Elastic Modulus	E	96.0	GPa
Poison ratio	ν	0.36	-
Yield strength	σ_y	930	MPa
Ultimate strength	σ_u	1070	MPa
Density	ρ	4620	kg/m^3

Fuselage Model Setup

The model setup of fuselage for the study involves following basic steps;

Mesh Generation and Convergence

A mesh sensitivity and convergence study was conducted, as per literature (Mubashir et al., 2024, Mubashir et al., 2022) prior to the main steps of analysis, to determine the optimal mesh size, significant to ensure the accuracy and computational efficiency. The convergence study was performed for all three design configurations. However, the summary of the corresponding results for only Design 3 using 09 different mesh sizes is presented in Table 3. The convergence study resulted to employ constant mesh size of 20 mm to bulkheads and stringers. A mesh size of 150 mm was selected to perform the final analysis as it yielded minimum error (less than 5%) in both deformation and stresses, depicted in Table 3. The final meshed model is illustrated in Figure 2.

Load and Boundary Conditions

Commonly, a fuselage consists of three parts; tail, cockpit and the cabin section. For present study, the research is focused on cabin section of fuselage with corrugated concept as used by Karthick et al (Karthick et al., 2013). Accordingly, at both end edges, fixed boundary conditions were applied (Figure 3). The load is applied in the form of pressure (62476 Pa) reported by Wang et al. (2021).

Path Definition

For obtaining the data points for graphs and identifying the variation along the wing span a path is generated on the skin using ANSYS path option available under construction geometry tool as shown in Figure 4.

Table 3. Mesh convergence study

Mesh Size (mm)	Deformation (mm)	Eq. Stress (MPa)	%age Difference Deformation	%age Difference (stress)
500	2.07	15.84	-	-
450	2.31	14.86	11.265	6.197
400	2.60	15.57	12.747	4.734
350	3.22	16.03	23.717	2.950
300	3.81	16.88	18.209	5.359
250	3.89	17.66	2.089	4.585
200	3.94	18.62	1.386	5.426
150	3.95	19.27	0.254	3.487
100	3.96	19.85	0.253	3.049

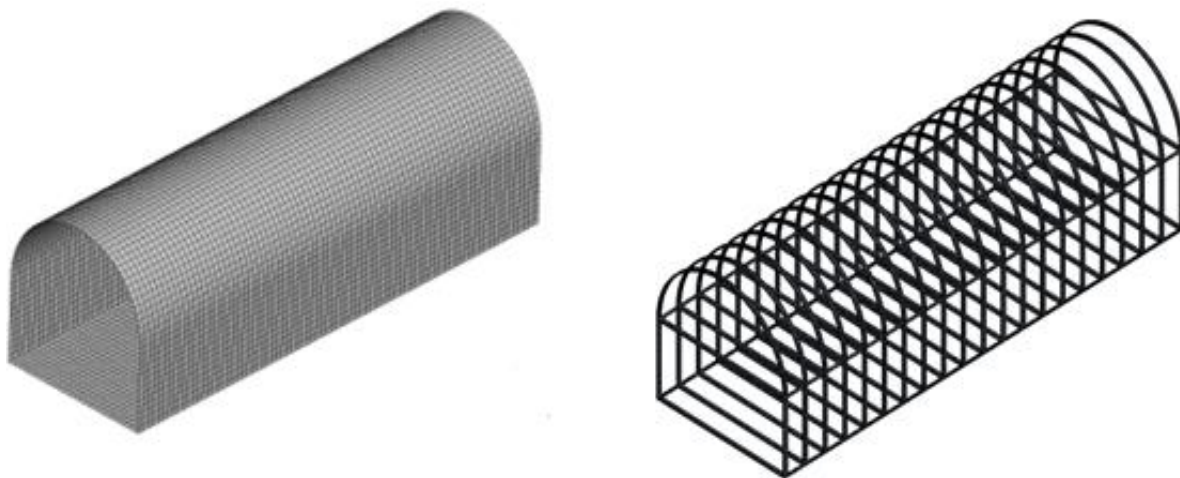


Figure 2. Meshed model fuselage skin and internal structure

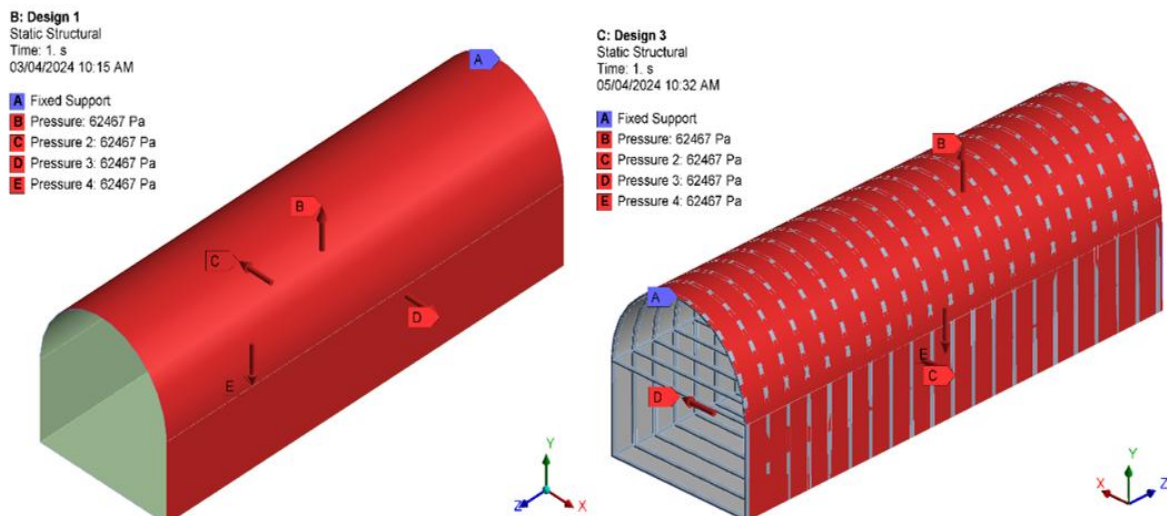


Figure 3. Boundary conditions used for fuselage analysis

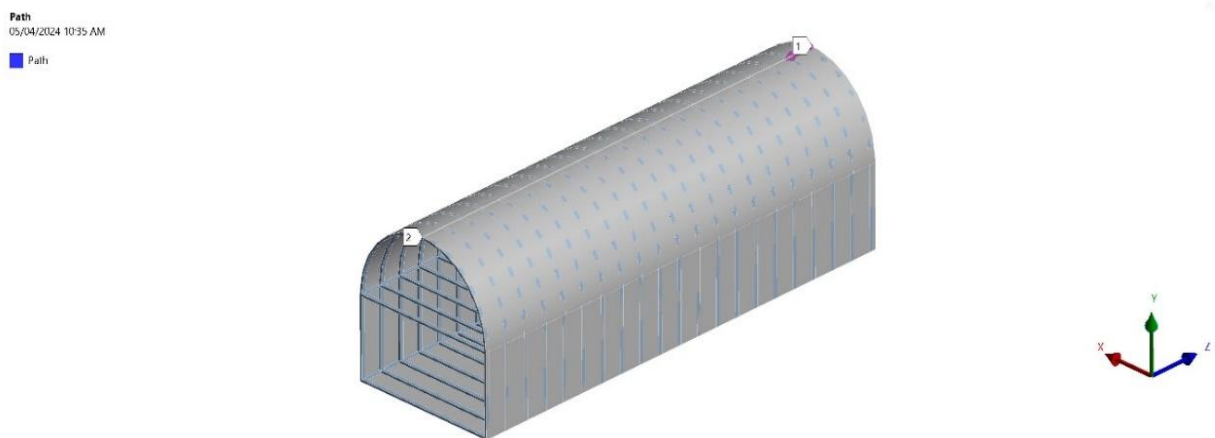


Figure 4. Path created along fuselage span

Results and Discussion

Fuselage Static Analysis Results

Deformation

The deformation analysis for all the three design configuration is presented in Figure 5 (a-c). Design 1 without any stiffening member shows a large amount of deformation have magnitude of 232.7 mm. It shows this deformation because of lack of internal stiffness and its own low thickness. Design 2 with bulkhead along the span direction also shows a moderate amount of deformation have magnitude of 65.03 mm. It shows this deformation because the addition of bulkhead increased the internal stiffness of skin and hence make it more rigid to resist the deformation under the applied load conditions.

Design 3 with bulkhead and stringers along the span direction also shows a moderate amount of deformation have magnitude of 54.56 mm. It shows this deformation because the addition of bulkhead and stringers increased the internal stiffness of skin and hence make it more rigid to resist the deformation under the applied load conditions. A graphical comparison between the variation of deformation along the fuselage span is presented in Figure 5 (d). The data points for the formation of graph are collected by using the scope option of path for deformation contour. The variation of deformation for all the three designs shows that deformation is maximum at the center of fuselage and minimum at both ends (Figure 6) that satisfied the applied boundary conditions (both end fixed) by ensuring the consistency with each other and literature.

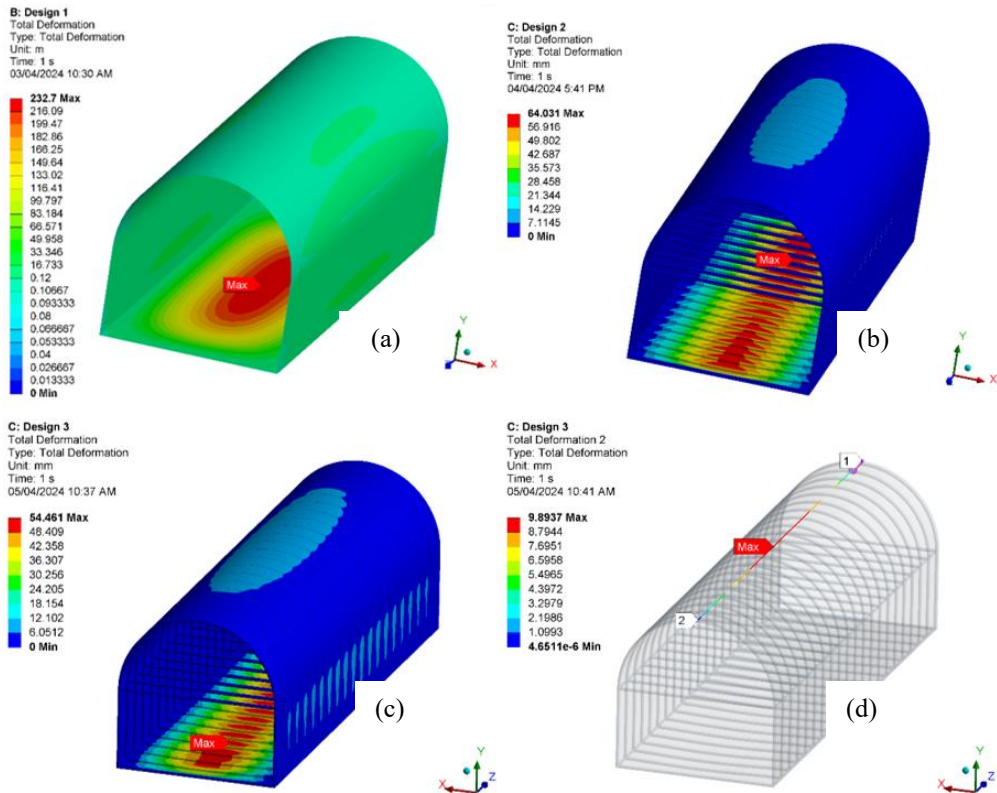


Figure 5. (a-c) Deformation evaluated for design 1,2 & 3 (d) Deformation contour along the path

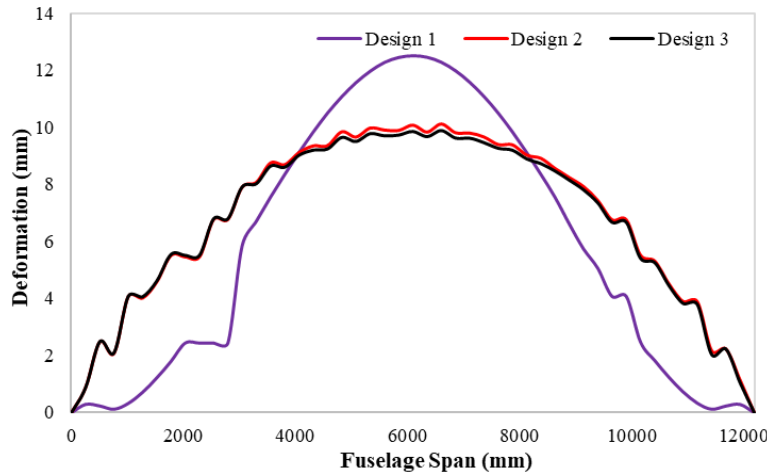


Figure 6. Variation of deformation along fuselage span for various designs

Equivalent Stress

The equivalent stress analysis is presented in Figure 7 (a-c). Design 1 without any stiffening member shows a large amount of stress have magnitude of 31123 MPa. It shows this stress because of lack of internal stiffness and its own low thickness and strength. Design 2 with bulkhead along the span direction also shows a moderate amount of stress have magnitude of 490 MPa. It shows this stress because the addition of bulkhead increased the internal strength of skin and hence prove it more strength to resist the stress under the applied load conditions. Design 3 with bulkhead and stringers along the span direction also shows a low amount of stress have magnitude of 400 MPa. It shows this stress because the addition of bulkhead and stringers increased the internal strength of skin and hence prove it more strength to resist the stress under the applied load conditions. A graphical comparison between the variation of stress along the fuselage span is presented in Figure 8. The data points for the formation of graph are collected by using the scope option of path for deformation contour as shown in Figure 7(d). The variation of stress for all the three designs shows that deformation is maximum at the center of fuselage and minimum at both

ends that satisfied the applied boundary conditions (both end fixed) by ensuring the consistency with each other and literature.

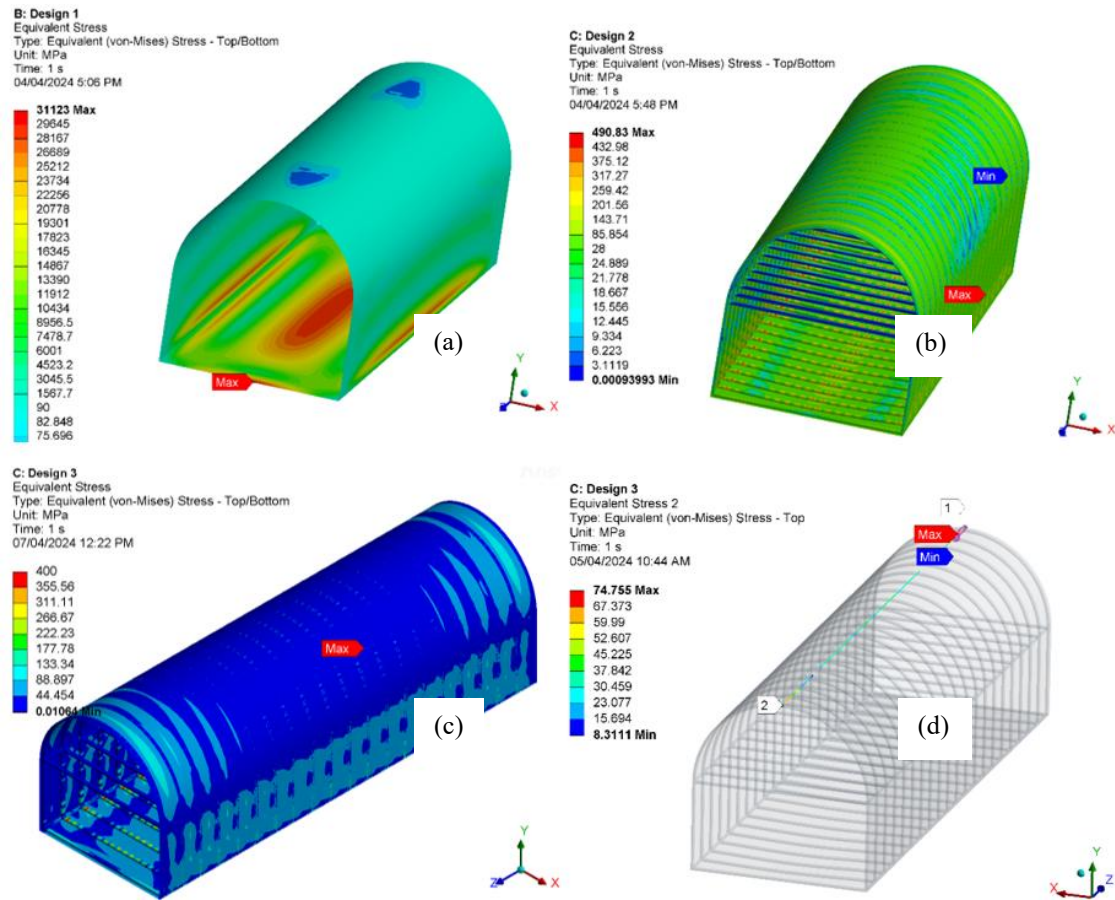


Figure 7. (a-c) Stress results for design 1,2 & 3 (d) Stress contour along the path

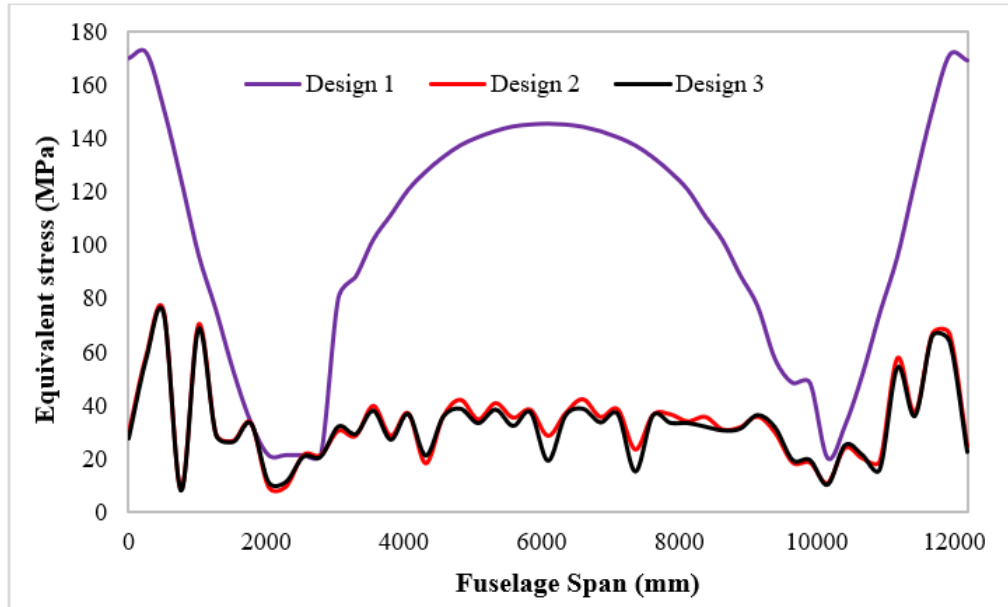


Figure 8. Variation of stress along fuselage span for various designs

Equivalent Strain

The results for equivalent strain are presented in Figure 9. The strain shows maximum magnitude in case of design 1 and minimum in case of design 3.

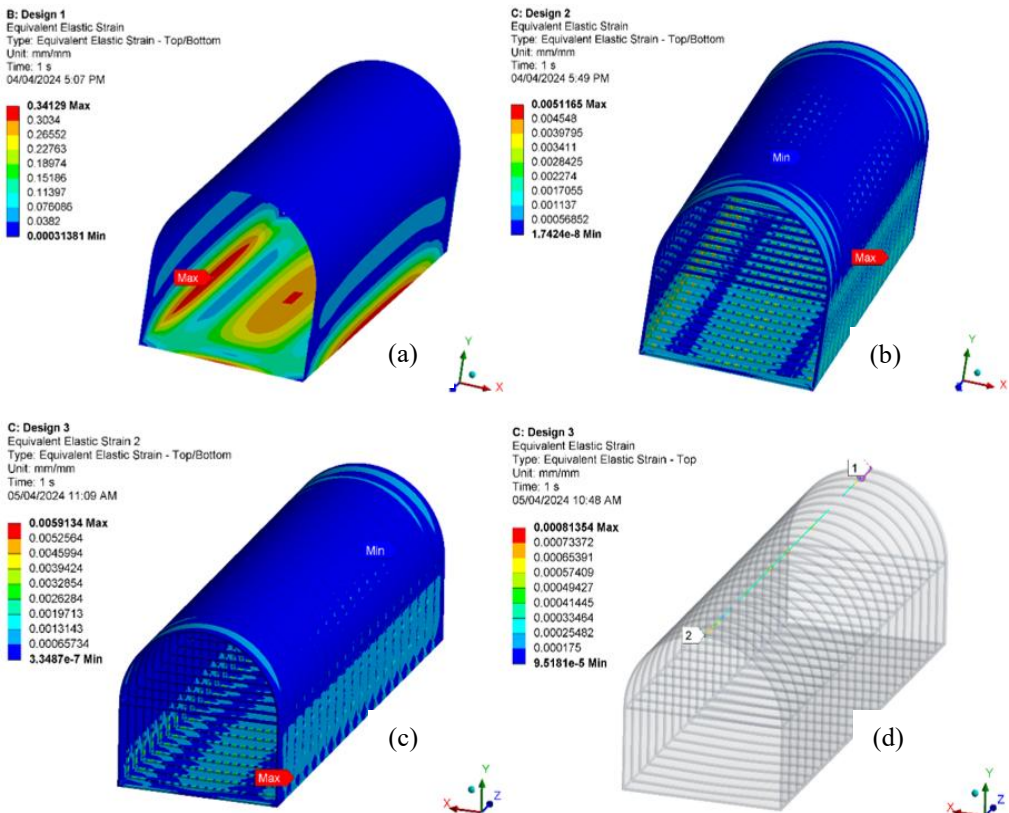


Figure 9. (a-c) Equivalent strain results for design 1,2 & 3 (d) Equivalent strain contour along the path

Factor of Safety (FOS)

The results for FOS contour for design configurations are presented in Figure 10. The FOS shows maximum magnitude of 2.32 in case of Design 3 and minimum magnitude of 0.03 in case of Design 1.

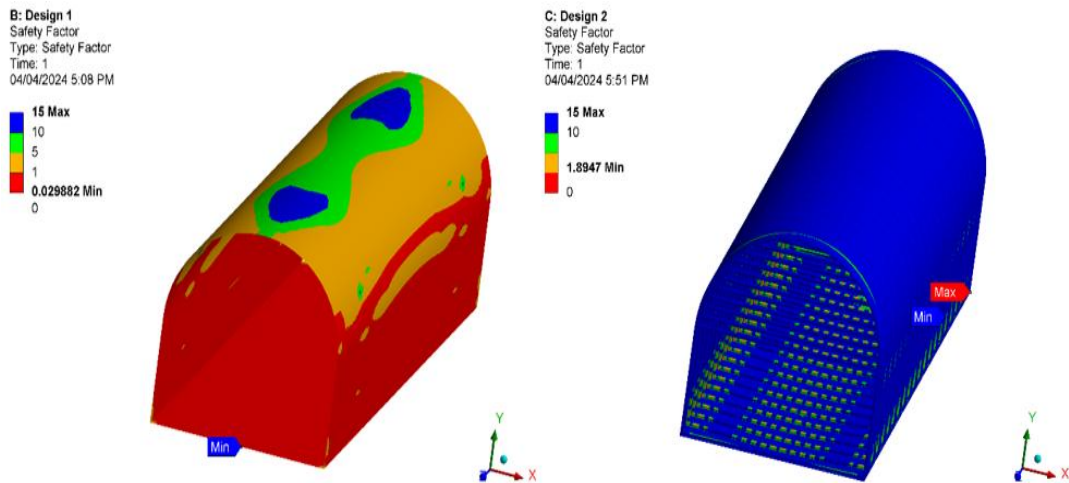


Figure 10. FOS contour design 1 and 2

Static Stress Results Summary

The overall summary of basic parameters obtained as an output in static analysis are presented in tabulated form in Table 4. The graphical comparison of FOS for all the designs in bar chart form is presented in Figure 11. Based on tabulated results and Figure 11 it can be concluded that Design 3 (one with bulkhead, skin and stringers) gives higher FOS, low stresses and deformation as compared to other.

Table 4. Comparison of various output parameters (fuselage)

Parameters	Design 1	Design 2	Design 3
Deformation (mm)	232.7	65.03	54.461
Stress (MPa)	31123	490.83	400
FOS	0.03	1.89	2.325

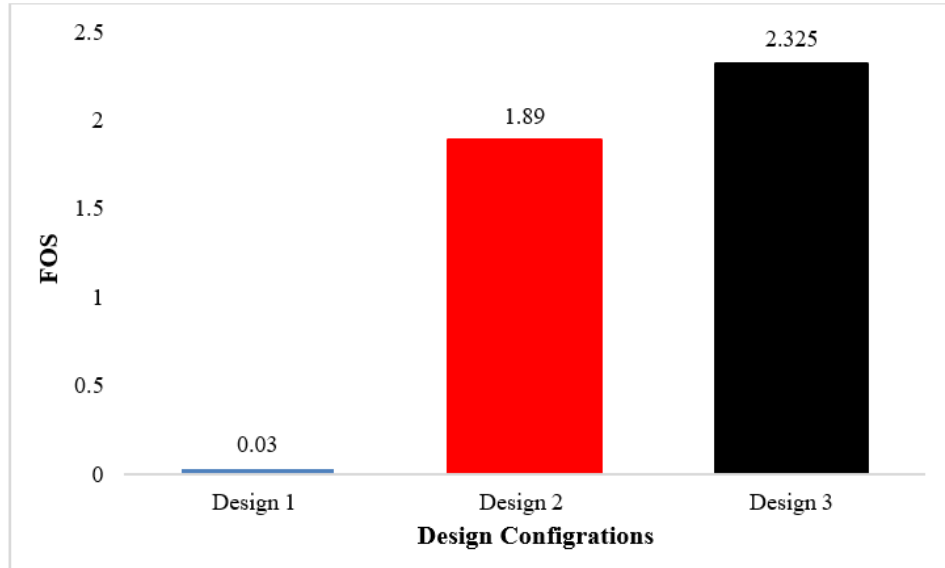


Figure 11. FOS comparison for various fuselage designs

The stress strain diagram for optimized design 2 and 3 are presented in figure 12. They show increasing straight line ensuring the accuracy of analysis performed because we assume only elastic properties during simulation and within elastic limit stress and strain graph must be straight line as predicted in figure 12.

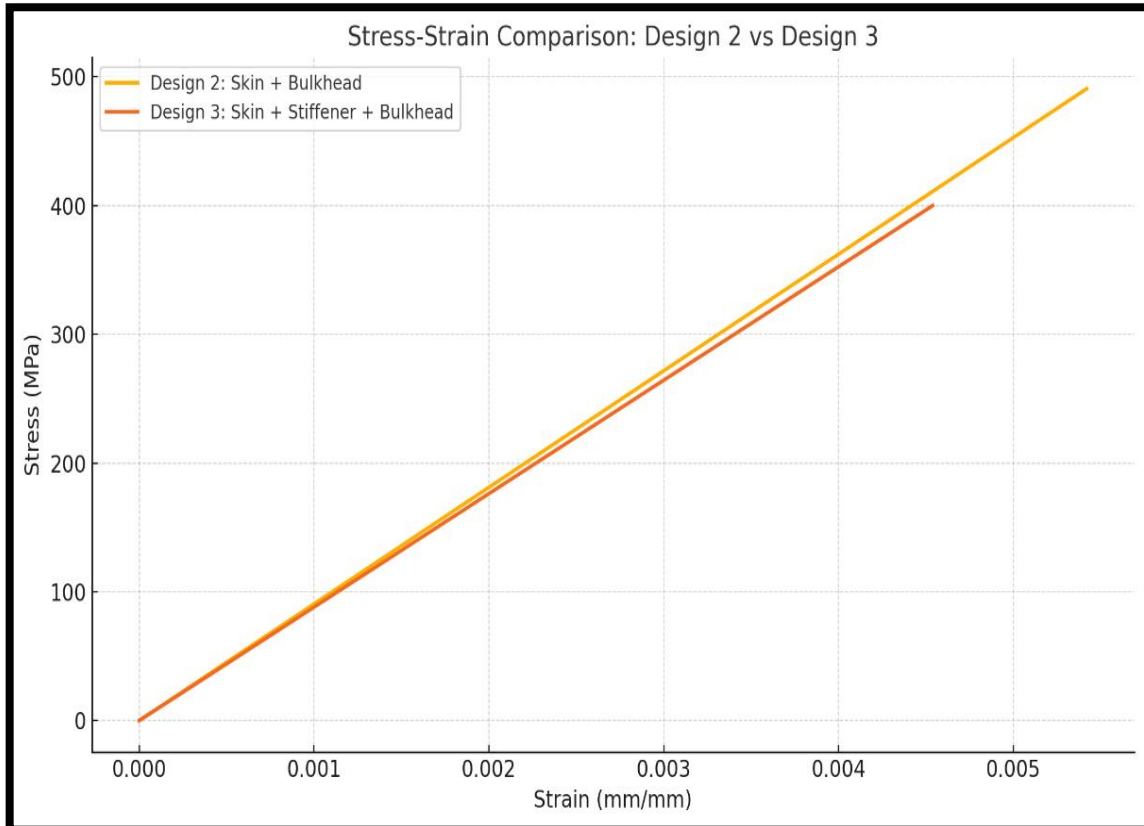


Figure 12. Stress strain diagram for design 2 and 3

Validation Study

The results of present study was validated by the existing research conducted by Veer et al (2022) in term of deformation and stress. It was found current study presented an optimized stress and deformation results as compared to literature. The tabulated comparision is present in table 5.

Table 5. Comparison of present results with literature

Parameters	Literature	Present	%age Improvement
Pressure Load (Pa)	62,467	62,467	-
Shear Stress (MPa)	131.2	127.54	2.78
Deformation (mm)	65.55	54.46	16.91

Fuselage Buckling Analysis Results

The results of fuselage buckling load factor for Design 1 are shown in Figure 12. All the multiplier are less than 1 that indicated skin will not able to withstand the applied load and buckled when this load will be applied in it. The results of wing buckling load factor for Design 2 and 3 are shown in Figure 13 and 14. All the multiplier are greater than 1 that indicated skin will able to withstand the applied load and will not buckled when this load will be applied in it.

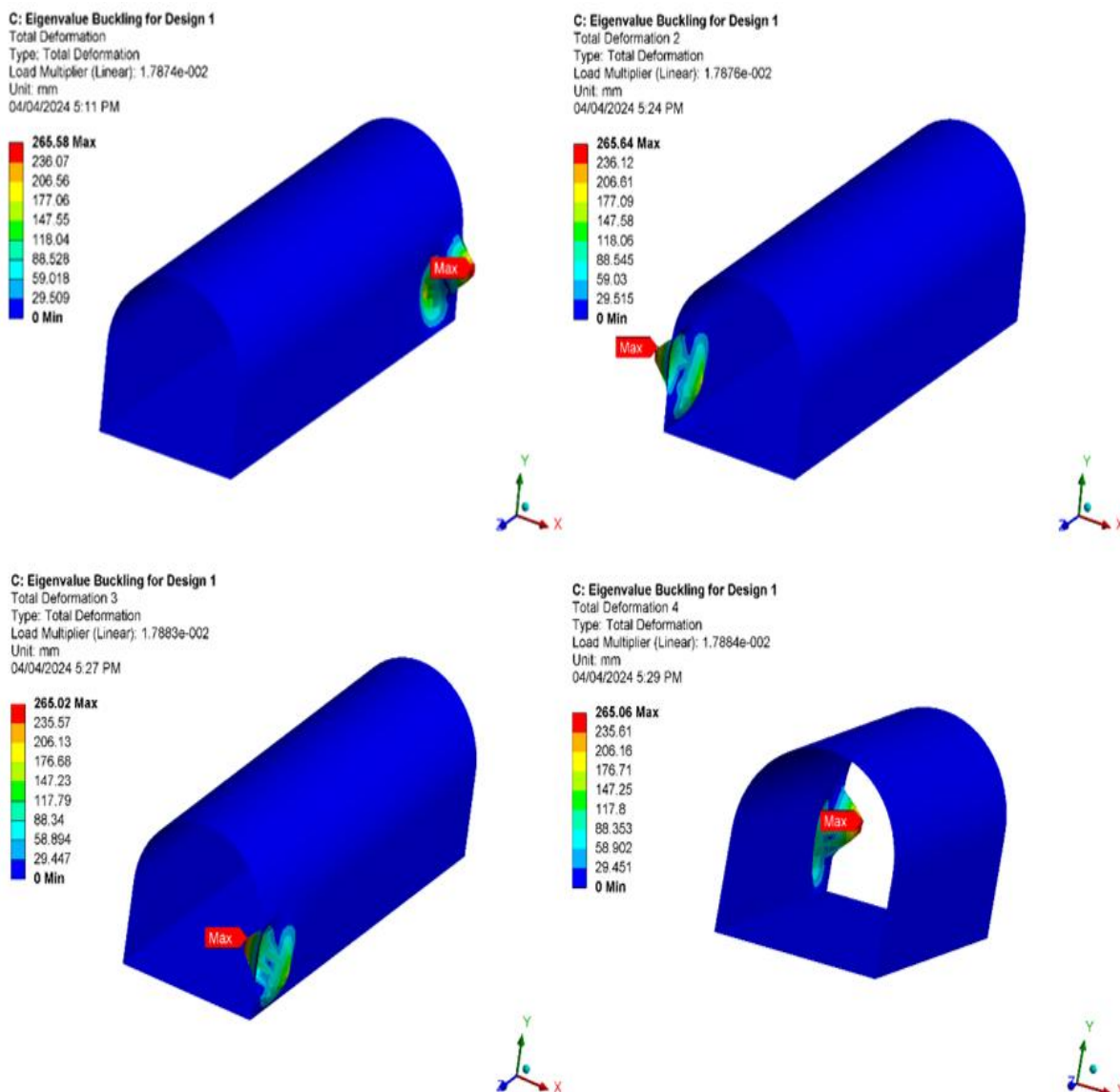


Figure 13. Buckling load multiplier for design 1

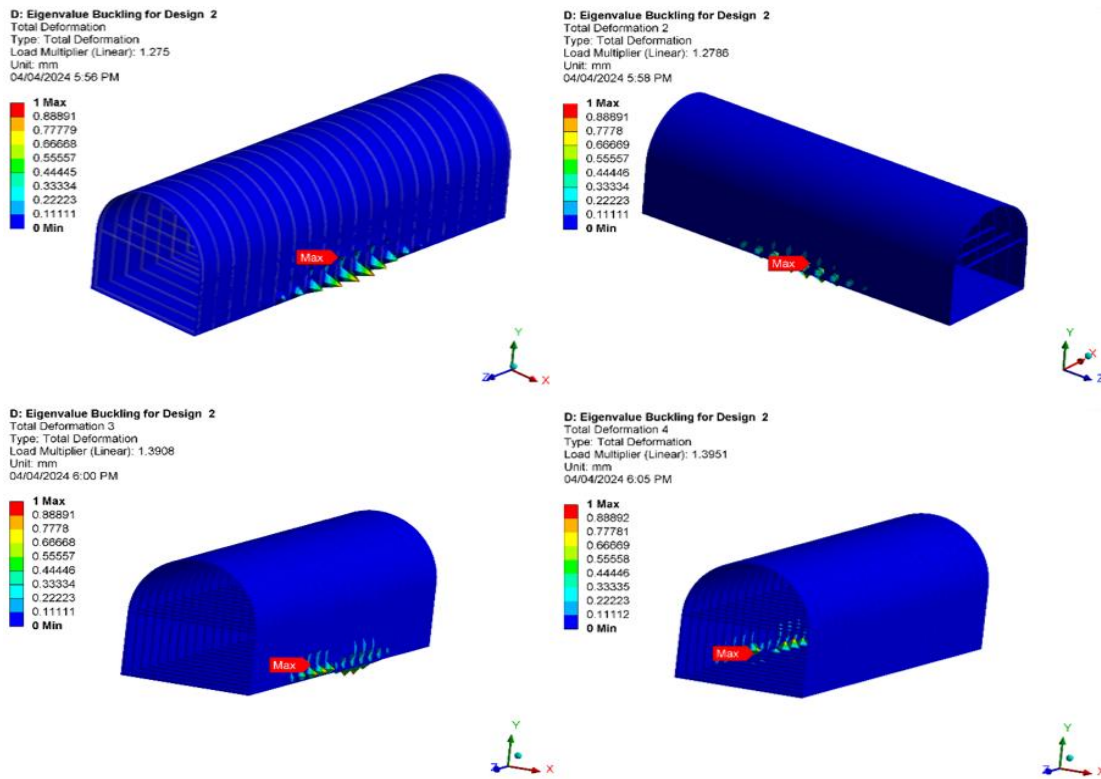


Figure 14. Buckling load multiplier for design 2

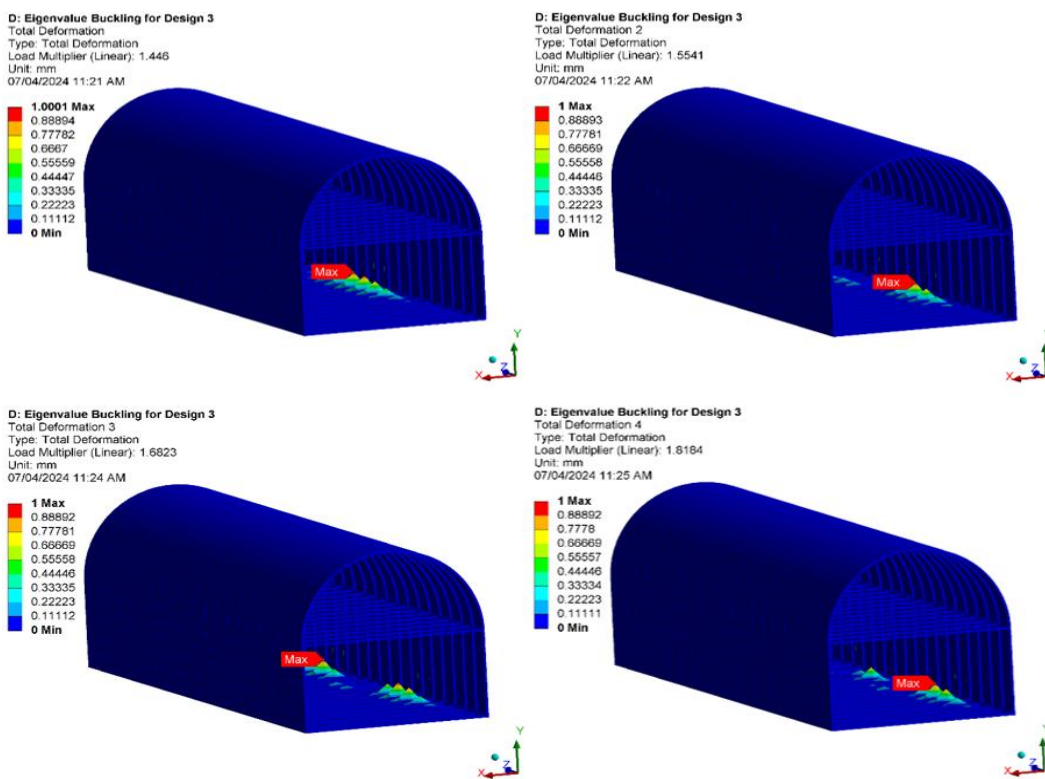


Figure 15. Buckling load multiplier for design 3

Buckling Analysis Results Summary

The summary of buckling load multiplier for first 4 modes in bar charts are presented in Figure 15. Based on Figure 15 it can be concluded that design 2 (one with bulkhead and skin) and design 3 (one with bulkhead, stringer

and skin) gives buckling load multiplier greater than one as compared to design 1 and can withstand the buckling effectively during the flight (Clint et al., 2014).

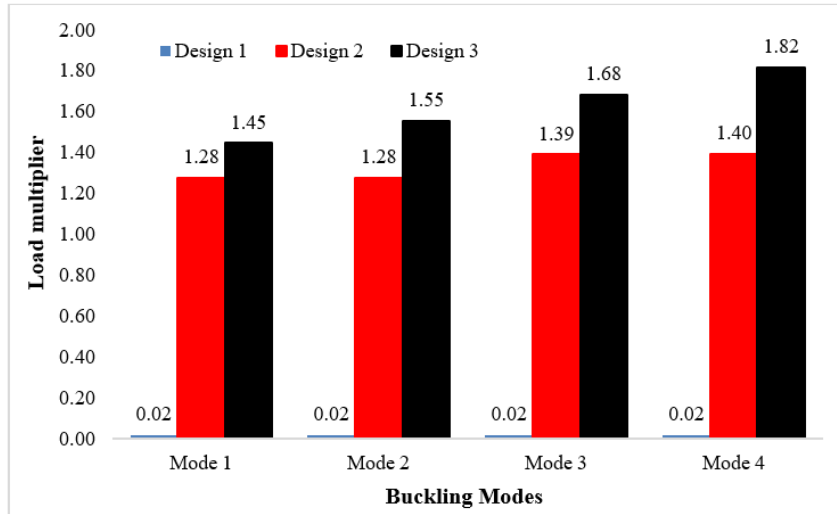


Figure 16. Buckling load multiplier comparison (fuselage)

Conclusion

The FEA results demonstrate the key role of internal stiffeners in corrugated plate fuselage structures. The unstiffened design (Design 1) had highest deformation and stresses under uniform pressure loading, resulting in lowest safety. Adding bulkheads (Design 2) reduced deformation and increased the buckling load, while the fully stiffened configuration (Design 3) demonstrated the best performance. The maximum von Mises stress was minimal and FoS was considerably higher in Design 3 than for the other cases. The buckling multiplier was greatest in case of Design 3, confirming that it can carry significantly higher-pressure loading. Design 3 shows significantly lower displacements and stress levels and provides the highest structural efficiency among the three Design configurations. The results agree with the established theory; longitudinal stringers efficiently stiffen the skin and bulkheads reduce the effective column length of the panel, improving the buckling capacity.

Recommendations

Future studies on these findings can be made by exploring the optimization of the corrugated plate fuselage geometry and layout of stiffeners. The structural behavior can be assessed under fatigue and dynamic loading. It would refine the fuselage designs for high performance, and light weight aerospace structures. In addition, this study only focused on uniform pressure loading, while a more complex pressure distribution alongwith lift and drag force calculated based on fluid structure interaction (FSI) approach can also be explored for future work.

Scientific Ethics Declaration

* The authors declare that the scientific ethical and legal responsibility of this article published in EPSTEM journal belongs to the authors.

Conflict of Interest

* The authors declare that they have no conflicts of interest.

Funding

*There is no funding

Acknowledgements or Notes

* This article was presented as a oral presentation at the International Conference on Engineering and Advanced Technology (ICEAT) held in Selangor, Malaysia on July 23-24, 2025.

References

Buehrle, R. D., Fleming, G. A., Pappa, R. S., & Grosveld, F. W. (2000). Finite element model development for aircraft fuselage structures. *Paper presented at the XVIII International Modal Analysis Conference*.

Clint, J., Kumar, S., & Shaik, N. J. (2014). Buckling analysis on aircraft fuselage structure skin. *International Journal of Engineering Development and Research*, 2(4), 3461–3474.

Hussain, S., & Chandan, R. (2016). Static and buckling analysis of center fuselage structure of a transport aircraft through FEA approach. *International Research Journal of Engineering and Technology*, 3(08), 1354–1357.

Karthick, B., Balaji, S., & Maniaraasan, P. (2013). Structural analysis of fuselage with lattice structure. *International Journal of Engineering Research*, 2, 1909–1913.

Madenci, E., & Guven, I. (2015). *The finite element method and applications in engineering using ANSYS®*. Springer.

Madier, D. (2020). *Practical finite element analysis for mechanical engineers* (Vol. 147). FEA Academy.

Mubashir, M., Mutahir, R., & Shoaib Ur Rehman, M. (2022). Design and analysis of hollow catenoidal horn profile for ultrasonic machining of composite materials. *Journal of Studies in Science and Engineering*, 2(2), 18–32.

Mubashir, M., Zaroor, A. K., Asim, A., & Shoaib-Ur-Rehman, M. (2024). A systematic framework for the design and material selection of composite for tennis racket upon impact. *Discover Materials*, 4(1), 57.

Peruru, S. P., & Abbisetti, S. B. (2017). Design and finite element analysis of aircraft wing using ribs and spars. *International Research Journal of Engineering and Technology*, 4(06), 2133–2139.

Raju, G., Suresh, V., Ramesh, T., & Hathiram, V. (2018). Modelling and analysis of fuselage. *International Research Journal of Advanced Technology*, 6(1), 204–212.

SatyanarayanaGupta, M., & Veeranjaneyulu, K. (2017). Fabrication and anayisis of adhesive joints used in aircraft structures. *Materials Today: Proceedings*, 4(8), 8279–8286.

Veeranjaneyulu, K., Sravanti, G., Kumar Chaturvedi, S., Joshi, S., & Kiran, K. S. (2022). Stress analysis of corrugated plate fuselage under different loading conditions. *Materials Today: Proceedings*, 64, 531–537.

Wang, X., Wang, D., Zhang, Y., & Wu, C. (2021). Research on the impact effect of AP1000 shield building subjected to large commercial aircraft. *Nuclear Engineering and Technology*, 53(5), 1686–1704.

Author(s) Information

Muhammad Mubashir

University of Engineering and Technology Lahore, G.T Road, Staff Houses Engineering University Lahore, Lahore, 39161, Pakistan

Contact e-mail: Mubashirmunir321@gmail.com

Mohsin Akhter

University of Engineering and Technology Lahore, G.T Road, Staff Houses Engineering University Lahore, Lahore, 39161, Pakistan

Qasim M.Turki

University of Al-Qadisiyah, Department of Materials Engineering, 58001 Al-Diwaniyah, Al-Qadisiyah, Iraq

Alaa Raad Hussein

University of Baghdad, Biomedical Engineering Department, Al-Khwarizmi College of Engineering, Baghdad, Iraq

Anas Asim

National Textile University, Department of Materials Sheikhupura - Faisalabad Rd, Mana Wala, Manawala, Pakistan

Shoaib Ur Rehman

University of Engineering and Technology, Lahore 54890, Pakistan

To cite this article:

Mubashir, M., Akhter, M., Turki, Q. M., Hussein, A. R., Asim, A., & Ur-Rehman, S. (2025). Buckling analysis of corrugated plate fuselage under uniform pressure loading condition. *The Eurasia Proceedings of Science, Technology, Engineering and Mathematics (EPSTEM)*, 37, 676-688.